

The Stellar IMF, Core Mass Function, & The Last-Crossing Distribution

Philip F. Hopkins¹*

¹*Department of Astronomy, University of California Berkeley, Berkeley, CA 94720*

Submitted to MNRAS, December, 2011

ABSTRACT

Hennebelle & Chabrier (2008) (HC08) attempted to derive the stellar IMF as a consequence of log-normal density fluctuations in a turbulent medium, using an argument similar to Press & Schechter (1974) for Gaussian random fields. Like that example, however, the solution there does not resolve the “cloud in cloud” problem; it also does not extend to the large scales that dominate the velocity and density fluctuations. In principle, these can change the results at the order-of-magnitude level or more. In this paper, we use the results from Hopkins (2011) (H11) to generalize the excursion set formalism and derive the exact solution in this regime. We argue that the stellar IMF and core mass function (CMF) should be associated with the *last-crossing* distribution, i.e. the mass spectrum of bound objects defined on the *smallest* scale on which they are self-gravitating. This differs from the *first-crossing* distribution (mass function on the largest self-gravitating scale) which is defined in cosmological applications and which H11 show corresponds to the GMC mass function in disks. We derive an analytic equation for the last-crossing distribution that can be applied for an arbitrary collapse threshold shape in ISM and cosmological studies. With this, we show that the *same* model that predicts the GMC mass function and large-scale structure of galaxy disks *also* predicts the CMF – and by extrapolation stellar IMF – in good agreement with observations. The only adjustable parameter in the model is the turbulent velocity power spectrum, which in the range $p \approx 5/3 - 2$ gives similar results. We also use this to formally justify why the approximate solution in HC08 is reasonable (up to a normalization constant) over the mass range of the CMF/IMF; however there are significant corrections at intermediate and high masses. We discuss how the exact solutions here can be used to predict additional quantities such as the clustering of stars, and embedded into time-dependent models that follow density fluctuations, fragmentation, mergers, and successive generations of star formation.

Key words: star formation: general — galaxies: formation — galaxies: evolution — galaxies: active — cosmology: theory

1 INTRODUCTION

The origin of the stellar initial mass function (IMF) is a question of fundamental importance for the study of star formation, stellar evolution and feedback, and galaxy formation. It is an input into a huge range of models of all of these phenomena, and a necessary assumption when deriving physical parameters from many observations. However, despite decades of theoretical study, it remains poorly understood. A critical first step – although by no means a complete description of the origin of the IMF – is understanding the origin and form of the mass function of protostellar cores (the CMF), specifically that of self-gravitating, collapsing cores that will ultimately form stars.

Recently, HC08 presented a compelling argument for the physical origin of the IMF shape, as a consequence of the CMF resulting from lognormal density fluctuations in a turbulent medium. It is increasingly clear that the density structure of the ISM is dominated by supersonic turbulence over a wide range of scales (e.g. Scalo & Elmegreen 2004; Elmegreen & Scalo 2004; Mac Low & Klessen 2004; McKee & Ostriker 2007), and a fairly generic consequence of this is that the density distribution converges towards a lognormal PDF, with a dispersion that scales weakly with Mach number (e.g. Vazquez-Semadeni 1994; Padoan et al. 1997; Scalo et al. 1998; Ostriker et al. 1999). Based on the analogy between

this and cosmological Gaussian density fluctuations, HC08, building on the earlier work in Inutsuka (2001) as well as Padoan et al. (1997); Padoan & Nordlund (2002), attempted to approximate the mass function of self-gravitating cores in a manner exactly analogous to Press & Schechter (1974). If the density field $\delta(\mathbf{x})$ (where $\delta \propto \ln \rho$) at the point \mathbf{x} is normally distributed, then the average δ smoothed around the point \mathbf{x} with the appropriate window function of effective radius R , $\delta(\mathbf{x}|R)$ is also normally distributed, with a variance $S = \sigma^2(R)$ that can (in principle) be calculated from the power spectrum or simply estimated from the Mach number (see e.g. Passot & Vazquez-Semadeni 1998; Nordlund & Padoan 1999; Federrath et al. 2008; Price et al. 2011). The total mass which is self-gravitating, over the scale R , is then just $\propto \int_{B(R)} \rho(\delta) P(\delta) d\delta$, where $B(R)$ is the critical density above which the region would be self-gravitating. Differentiating this total mass fraction with respect to the mass scale associated with each R gives – approximately – the total mass in bound objects per unit mass, $M^2 dN/dM$, hence the mass function. HC08 showed that, for plausible S , and B given by the Jeans condition for thermal plus turbulent velocities, this argument reproduces all of the key features of the observed CMF and stellar IMF (for extensions of this calculation allowing for different gas properties and , see Hennebelle & Chabrier 2009, 2011; Chabrier & Hennebelle 2011).

While extremely interesting, there are, however, a number of uncertain assumptions in this derivation of the CMF. Because it focuses on small scales exclusively, the properties of the “parent”

* E-mail: phopkins@astro.berkeley.edu

scales (e.g. GMCs) must be assumed somewhat ad hoc. Since most of the power in velocity (hence density) fluctuations is on large scales (true for any reasonable turbulent power spectrum, and also observed; see Ossenkopf & Mac Low 2002; Brunt et al. 2009), this means $S(R)$ could also not be calculated but was instead assumed, and its “run” with radius R (being undetermined) was neglected (and the resulting mass function artificially truncated before going to very large scales).

Most important, like Press & Schechter (1974), this derivation does not resolve the “cloud in cloud” problem. A given region may well be self-gravitating on many different scales R (the smoothed $\delta(\mathbf{x}|R)$ crossing back and forth across the critical $B(R)$ with scale). This makes the resulting mass function inherently ambiguous, since different crossings of the same spatial location are counted multiple times and with different signs. Bond et al. (1991) resolved this ambiguity by extending the mathematical excursion set formalism and defining the “first crossing distribution.” This allowed them to rigorously calculate the mass function of objects – counting each point only once – where “mass” was defined as the mass enclosed in the *largest* scale R on which a region was self-gravitating.

More recently, H11 showed how the full excursion set formalism could be generalized to the problem of lognormal density fluctuations in a gaseous galactic disk. By including disk scale-effects, they showed that it is also possible to predict the absolute mass scales, variance $\sigma^2(R)$, and barrier $B(R)$ – quantities which had to be assumed *ad hoc* in HC08 – with only the assumption of a turbulent spectral shape. On small scales (below the disk scale height), the collapse condition is just the Jeans condition for turbulent plus thermal support – identical to HC08 – so there is no reason why the approach therein cannot be extended to the same scales.

H11 showed that the first-crossing distribution for turbulent gas in a galaxy disk is *not* the CMF or stellar IMF, but rather agrees extremely well with observations of the mass function and other properties of giant molecular clouds (GMCs). This highlights just how important the distinction of multiple crossings can be – extending the HC08 argument to large scales, self-gravitating objects with scales $\sim 10^6 M_\odot$ would be recovered (and contain more mass than the objects self-gravitating on scales $\sim 1 M_\odot$). Clearly, these are the “parent” clouds, not the protostellar cores!

So how can the two be distinguished? Physically, consider a region which is self-gravitating on a large scale R_0 . If it contains multiple sub-regions that are themselves self-gravitating on a smaller scale R_1 , then the entire R_0 object will not form a single core (see e.g. the discussion of the “cloud in cloud” problem in Veltchev et al. 2011; Donkov et al. 2011). Since the mean density at R_1 to be self-gravitating must be larger than that at R_0 , these sub-regions will collapse more rapidly – the “parent cloud” is fragmenting into smaller objects. This can be continued iteratively inside R_1 . It is only when a region is self-gravitating on a scale R_ℓ , and *not* self-gravitating on any smaller scales, that its collapse will proceed without fragmentation.

Therefore, we argue in this paper that the CMF (and, to the extent that it is related, the IMF) should be associated with the *last-downcrossing* distribution: i.e. the mass function of regions which are self-gravitating, but with mass defined at the smallest scales on which they are self-gravitating. This has not, to our knowledge, been studied in any cosmological context (since halos are assumed to collapse “into” the mass they contain), so in § 2, we derive a rigorous analytic expression for this mass function as a function of arbitrary collapse threshold. In § 3 we combine this with the model from H11, which gives the appropriate collapse threshold and variance for a galactic disk. In § 4 we compare the results to

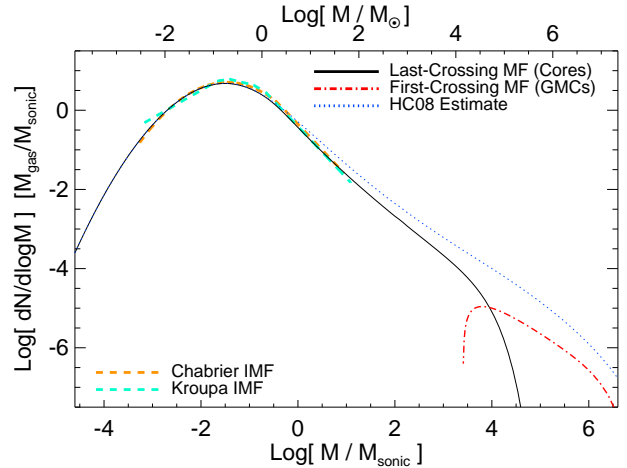


Figure 1. Predicted last-crossing mass function (distribution of bound masses measured on the *smallest* scale on which they are self-gravitating) for a galactic disk with turbulent spectral index $p = 2$, and Mach number at scale $\sim h$ of $\mathcal{M}_h = 30$. In units of the sonic mass $M_{\text{sonic}} \equiv (2/3) c_s^2 R_{\text{sonic}}/G$ and total disk gas mass M_{gas} , all other properties are completely specified by disk stability. We calculate this with the analytic iterative solution to Eq. 14; the standard Monte Carlo excursion set method gives an identical result. We compare the first-crossing distribution – the distribution of masses measured on the *largest* scale on which gas is self-gravitating, which in H11 we show agrees extremely well with observed GMC mass functions. The MF derived in HC08 by ignoring multiple crossings is also shown. We compare the observed stellar IMF from Kroupa (2002) and Chabrier (2003) (shifted to higher masses by a simple core-to-stellar mass factor of 3).

the observed CMF and stellar IMF, see how it contrasts with the first-crossing distribution (GMC mass function), and examine its dependence on turbulent properties. In § 6 we discuss implications and future directions for this work.

2 THE LAST-DOWNCROSSING DISTRIBUTION

Our derivation here closely follows that of the first-crossing distribution in Zhang & Hui (2006), to whom we refer for more details.

Consider the Gaussian field $\delta(\mathbf{x}|R)$ (which for this problem represents the logarithmic density field smoothed in a kernel of radius R about \mathbf{x}); the variance in the field $\equiv S(R)$ is a monotonically decreasing function of R so we can take S as the independent variable and consider $\delta(\mathbf{x}|S)$. For convenience we will drop the explicit notation of \mathbf{x} . The PDF of $\delta(S)$ is just

$$P_0(\delta|S) = \frac{1}{\sqrt{2\pi S}} \exp\left(-\frac{\delta^2}{2S}\right) \quad (1)$$

The barrier $B(S)$ is the minimum value $\delta(S)$ which defines objects of interest (e.g. collapsing regions). Normally, we would define the first-crossing distribution by beginning with the initial condition $\delta(0) = 0$ at $S = 0$ ($R \rightarrow \infty$), then evaluating $\delta(S)$ at successively increasing S (smaller scales R). This is straightforward: given an “initial” value $\delta_0(S_0)$ at scale S_0 , the probability of a value $\delta_1(S_1)$ at a scale $S_1 > S_0$ is just

$$P_{10}[\delta_1(S_1) | \delta_0(S_0)] = P_0(\delta_1 - \delta_0 | S_1 - S_0). \quad (2)$$

This can be integrated until the “trajectory” (or random walk) $\delta(S)$ first exceeds $B(S)$.

For the last crossing distribution, we need to determine the smallest scale at which a trajectory that had previously crossed the

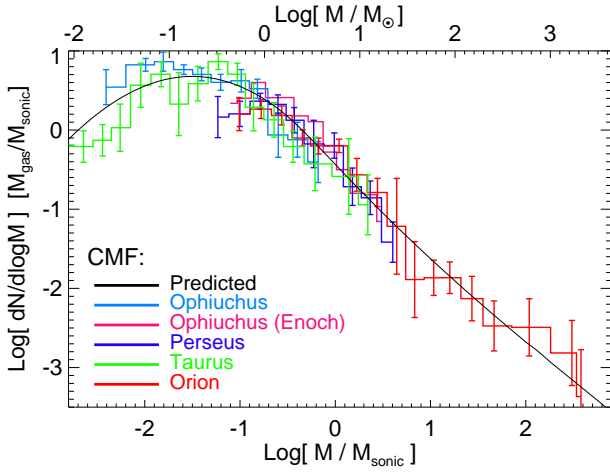


Figure 2. Predicted last-crossing mass function from Fig. 1, compared to observed pre-stellar/starless core MFs in different regions. The CMFs for Ophiuchus, Perseus, Taurus, and Orion are compiled in Sadavoy et al. (2010); we also compare the independent determination for Ophiuchus in Enoch et al. (2008). The CMFs in the Pipe (Rathborne et al. 2009) and Chameleon I (Belloche et al. 2011) also agree well but would be indistinguishable from the other systems on this plot. The normalization of the observed/predicted CMF is arbitrary (depending on absolute mass and volume) but – unlike the comparison with the stellar IMF – the absolute mass value is not rescaled here. Note the dynamic range is limited, and the observations have substantial uncertainties, but the agreement is good.

barrier at some larger scale again falls below $B(S)$. Consider a trajectory, therefore, in the opposite direction: beginning at an initial $\delta_i(S_i)$ at some arbitrarily small $R_i \rightarrow 0$, with a corresponding $S_i(R_i)$, and evaluating δ at successively smaller S (larger R). For the last-crossing distribution to be meaningfully defined, it must be the case that as $R \rightarrow 0$, the probability of δ_i exceeding $B(S_i)$ vanishes, $P_0(B[S_i] | S_i) \rightarrow 0$.

Define the last crossing distribution $f_\ell(S | \delta_i) dS$ as the probability that a trajectory, beginning from this state, crosses $B(S)$ for the first time between S and $S + dS$. Also define $\Pi(\delta | \delta_i, S) d\delta$ as the probability for the trajectory beginning at $\delta_i(S_i)$ to have a value between δ and $\delta + d\delta$ at scale S , *without* having crossed $B(S)$ at any larger S . Clearly, the integral of f_ℓ and integral of Π for $\delta < B(S)$ must sum to unity:

$$1 = \int_S^{S_i} dS' f_\ell(S' | \delta_i) + \int_{-\infty}^{B(S)} \Pi(\delta | \delta_i, S) d\delta \quad (3)$$

For a step in this “opposite” direction of decreasing S , the probability of going from an initial $\delta_1(S_1)$ to a value $\delta_0(S_0)$ with $S_1 > S_0$ is related to the probability of going from $\delta_0(S_0)$ to $\delta_1(S_1)$ by Bayes’s theorem:

$$P_{01}[\delta_0(S_0) | \delta_1(S_1)] = P_{10}[\delta_1(S_1) | \delta_0(S_0)] \frac{P_0(\delta_0 | S_0)}{P_0(\delta_1 | S_1)} \\ = P_0[\delta_0 - \delta_1(S_0/S_1) | (S_1 - S_0)(S_0/S_1)] \quad (4)$$

If we ignored the barrier, $\Pi(\delta | \delta_i, S)$ would be equal to $P_{01}[\delta(S) | \delta_i(S_i)]$. But we must subtract from this the probability that a trajectory crosses the barrier at some larger $S' > S$ and then passes through $\delta(S)$, so

$$\Pi(\delta | \delta_i, S) = P_{01}[\delta(S) | \delta_i(S_i)] - \int_S^{S_i} dS' f_\ell(S' | \delta_i) P_{01}[\delta(S) | \delta'(S') = B(S')] \quad (5)$$

Before going further, note that we do not know the value of $\delta_i(S_i)$, but know its distribution. The fraction of trajectories crossing the barrier at each S is the integral of $f_\ell(S | \delta_i)$ weighted by the distribution of δ_i . We therefore define

$$f_\ell(S) \equiv \langle f_\ell(S | \delta_i) \rangle = \int_{-\infty}^{\infty} d\delta_i P_0(\delta_i | S_i) f_\ell(S | \delta_i) \quad (6)$$

Technically, the upper limit of this integral should be $B(S_i)$, since the trajectory must begin as uncollapsed, but since we choose S_i such that the collapsed fraction is vanishingly small, we can safely take $B(S_i) \rightarrow \infty$. If we take the integral $\int_{-\infty}^{\infty} d\delta_i P_0(\delta_i | S_i)$ with respect to both sides of Equation 3, note that both δ and S' are independent of δ_i , and use the fact that

$$\int_{-\infty}^{\infty} d\delta_i P_0(\delta_i | S_i) P_{01}[\delta(S) | \delta_i(S_i)] = P_0(\delta | S) \quad (7)$$

we obtain the δ_i -averaged equations

$$1 = \int_S^{S_i} dS' f_\ell(S') + \int_{-\infty}^{B(S)} \Pi(\delta | S) d\delta \quad (8)$$

$$\Pi(\delta | S) = P_0(\delta | S) - \int_S^{S_i} dS' f_\ell(S') P_{01}[\delta(S) | B(S')] \quad (9)$$

Taking the derivative of Eq. 8, we obtain

$$f_\ell(S) = \Pi(B(S) | S) \frac{dB}{dS} + \int_{-\infty}^{B(S)} \frac{\partial \Pi(\delta | S)}{\partial S} d\delta \quad (10)$$

Finally, we insert Eq. 9 in Eq. 10, perform some simplifying algebra¹ and obtain

$$f_\ell(S) = g_1(S) + \int_S^{S_i} dS' f_\ell(S') g_2(S, S') \quad (14)$$

where

$$g_1(S) = \left[2 \frac{dB}{dS} - \frac{B(S)}{S} \right] P_0(B(S) | S) \quad (15)$$

$$g_2(S, S') = \left[\frac{B(S) - B(S')}{S - S'} + \frac{B(S)}{S} - 2 \frac{dB}{dS} \right] P_{01}[B(S) | B(S')] \quad (16)$$

Equation 14 is a Volterra integral equation, which for a general barrier $B(S)$ has a unique solution that can be calculated by standard numerical methods. For example, if we grid S on a mesh with equal spacing,

$$S_n = S_i - n \Delta S, \quad n = 0, 1, \dots, N, \quad \Delta S = \frac{S_i - S}{N} \quad (17)$$

and treat $f_\ell(S_n)$ as a vector, then the integral equation becomes a

¹ Specifically, using the relations

$$\left[\int_{-\infty}^{B(S)} d\delta P_{01}[\delta(S) | B(S')] \right] \Big|_{S' \rightarrow S} = \frac{1}{2} \quad (11)$$

$$\int_{-\infty}^{B(S)} \frac{\partial P_0(\delta | S)}{\partial S} d\delta = -\frac{B(S)}{2S} P_0(B(S) | S) \quad (12)$$

$$\int_{-\infty}^{B(S)} \frac{\partial P_{01}[\delta(S) | B(S')]}{\partial S} d\delta = \\ - \left[\frac{B(S') - B(S)}{2(S' - S)} + \frac{B(S)}{2S} \right] P_{01}[B(S) | B(S')] \quad (13)$$

triangular matrix equation which can be solved iteratively:

$$f_\ell(S_0) = g_1(S_0) = 0 \quad (18)$$

$$f_\ell(S_1) = g_1(S_1) (1 - H_{1,1})^{-1} \quad (19)$$

$$f_\ell(S_n)|_{n>1} = \frac{g_1(S_n) + f_\ell(S_{n-1})H_{n,n} + \sum_{m=1}^{n-1} [f_\ell(S_m) + f_\ell(S_{m-1})]H_{n,m}}{1 - H_{n,n}} \quad (20)$$

where

$$H_{n,m} = \frac{\Delta S}{2} g_2 \left[S_n, S_m + \frac{\Delta S}{2} \right] \quad (21)$$

For a linear barrier, $B(S) = B_0 + \beta S$, this has a closed-form solution:

$$f_\ell(S|B = B_0 + \beta S) = \beta P_0(B(S)|S) = \frac{\beta}{\sqrt{2\pi S}} \exp\left(-\frac{B^2}{2S}\right) \quad (22)$$

Equation 14 is qualitatively similar to the governing equation for the first-crossing distribution (compare Eq. 5 in Zhang & Hui 2006), but with some critical differences. Up to a sign, $g_1(S)$ is identical. In the g_2 term, however, there is an additional $B(S)/S$ in the coefficient, and $P_{01}[B(S)|B(S')]$ appears instead of $P_{10}[B(S)|B(S')]$. And of course, the integration proceeds in the opposite direction. These corrections result in qualitatively different behavior. For example, for the linear barrier, the first-crossing distribution has a pre-factor B_0/S instead of β ; for a constant barrier ($\beta = 0$), the first-crossing distribution is well-defined but the last-crossing distribution vanishes because there are continued crossings on all scales as $S \rightarrow S_i$.

3 THE CORE MASS FUNCTION: RIGOROUS SOLUTIONS

We have now derived the rigorous solution for the number of bound objects per interval in mass M , defined as the mass on the *smallest* scale on which they are self-gravitating. To apply this to a physical system, we need the collapse barrier $B(S)$ and variance $S = \sigma^2(R) = \sigma^2(M)$. In HC08, $B(S)$ is defined by the Jeans overdensity $\rho_{\text{crit}}(R) > (c_s^2 + v_t^2(R))/4\pi G$, but the normalization of the background density, c_s , and v_t is essentially arbitrary. Moreover, S is not derived, but a simple phenomenological model is used, and the authors avoid uncertainties related to this by dropping terms with a derivative in S . In H11, we show how $S(R)$ and $B(S)$ can be derived self-consistently on all scales for a galactic disk. For a given turbulent power spectrum, together with the assumption that the disk is marginally stable ($Q = 1$), $S(R)$ can be calculated by integrating the contribution from the velocity variance on all scales $R' > R$:

$$S(R) = \int_0^\infty \sigma_k^2(\mathcal{M}[k]) |W(k, R)|^2 d \ln k \quad (23)$$

$$\sigma_k^2 = \ln \left[1 + \frac{3}{4} \frac{v_t^2(k)}{c_s^2 + \kappa^2 k^{-2}} \right] \quad (24)$$

where W is the window function for the density smoothing (for convenience, we take this to be a k -space tophat inside $k < 1/R$). This is motivated by and closely related to the correlation between Mach number and dispersion in turbulent box simulations (see Padoan et al. 1997; Passot & Vazquez-Semadeni 1998; Federrath et al. 2008; Price et al. 2011). $B(R)$ is properly given by

$$B(R) = \ln \left(\frac{\rho_{\text{crit}}}{\rho_0} \right) + \frac{S(R)}{2} \quad (25)$$

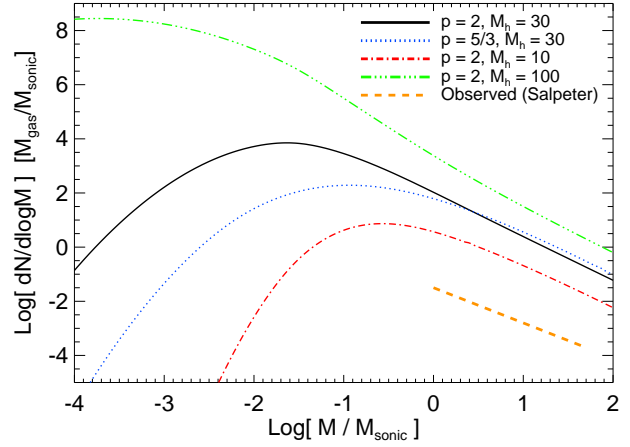


Figure 3. Variation in the predicted CMF/last-crossing MF with model assumptions. We compare the standard model from Fig. 1 ($p = 2$, $\mathcal{M}_h = 30$). Raising/lowering \mathcal{M}_h substantially slows/steepens the cutoff below the sonic mass. Assuming $p = 5/3$ (at fixed \mathcal{M}_h) also slows this cutoff. These variations have almost no effect on the high-mass slope, which is close to Salpeter in all cases.

$$\frac{\rho_{\text{crit}}}{\rho_0} \equiv \frac{Q}{2\tilde{\kappa}} \left(1 + \frac{h}{R} \right) \left[\frac{\sigma_g^2(R)}{\sigma_g^2(h)} \frac{h}{R} + \tilde{\kappa}^2 \frac{R}{h} \right] \quad (26)$$

where ρ_0 is the mean midplane density of the disk, $\tilde{\kappa} = \kappa/\Omega = \sqrt{2}$ for a constant- V_c disk, and

$$\sigma_g^2(R) = c_s^2 + v_A^2 + \langle v_t^2(R) \rangle \quad (27)$$

The mapping between radius and mass is

$$M(R) \equiv 4\pi \rho_{\text{crit}} h^3 \left[\frac{R^2}{2h^2} + \left(1 + \frac{R}{h} \right) \exp\left(-\frac{R}{h}\right) - 1 \right] \quad (28)$$

It is easy to see that on small scales, these scalings reduce to the Jeans criterion for a combination of thermal (c_s), turbulent (v_t), and magnetic (v_A) support, with $M = (4\pi/3) \rho_{\text{crit}} R^3$; on large scales it becomes the Toomre criterion with $M = \pi \Sigma_{\text{crit}} R^2$.

Finally, we note that because the trajectories $\delta(\mathbf{x}|R)$ defined above sample the Eulerian volume, the mass function is given by

$$\frac{dn}{dM} = \frac{\rho_{\text{crit}}(M)}{M} f_\ell(M) \left| \frac{dS}{dM} \right| \quad (29)$$

It is worth noting that, with $S(R)$ and $B(R)$ derived above, there are only two free parameters that together completely specify the model in dimensionless units. These are the spectral index p of the turbulent velocity spectrum, $E(k) \propto k^{-p}$ (usually in the narrow range $p \approx 5/3 - 2$), and its normalization, which we parameterize as the Mach number on large scales $\mathcal{M}_h^2 \equiv \langle v_t^2(h) \rangle / (c_s^2 + v_A^2)$. Of course, we must specify the dimensional parameters h (or c_s) and ρ_0 to give absolute units to the problem, but these simply rescale the predicted quantities.

4 RESULTS

Using these relations, we are now in a position to calculate the last-crossing mass function. Figure 1 shows the results of calculating the last-crossing distribution $f_\ell(S)$ for typical parameters $p = 2$ (Burgers' turbulence, typical of highly super-sonic turbulence) and $\mathcal{M}_h = 30$ (typical for GMCs). First, we can confirm our analytic derivation in Eq. 14. It is easy to calculate the last-crossing distribution by generating a Monte Carlo ensemble of trajectories $\delta(R)$ in the standard manner of the excursion set formalism (beginning

at $R \rightarrow \infty$ and $S = 0$), and the details of this procedure are given in H11; here we simply record the last down-crossing for each trajectory and construct the mass function. The result is statistically identical to the exact solution. However, below the “turnover” in the last-crossing mass function, the Monte Carlo method becomes extremely expensive and quite noisy, because an extremely small fraction of the total galaxy *volume* is in low-mass protostellar cores (sampling $\ll 0.1 M_{\text{sonic}}$ requires $\sim 10^{10}$ trajectories).

We compare the last-crossing mass function to the predicted first-crossing distribution – i.e. the mass function of bound objects defined on the *largest* scale on which they are self-gravitating. The two are strikingly different: they have different shapes, different power-law slopes, and the “characteristic masses” are separated by more than six orders of magnitude! Clearly, it is critical to rigorously address the “cloud in cloud” problem when attempting to define either.

Physically, in H11 we argue that the first-crossing distribution should be associated with the mass function of GMCs, and show that it agrees very well with observations of the same. The last-crossing distribution, on the other hand, should correspond to the proto-stellar core MF – and by extension to the stellar IMF (although that conversion is uncertain and may well be mass-dependent, as discussed below). We see that here. As shown with the approximate derivation in HC08, the exact predicted mass function reproduces all of the key observed features of the core/stellar MF. The high-mass behavior is an approximate power-law with a Salpeter-like slope $dN/dM \propto M^{-\alpha}$ with α slightly larger than 2; at lower masses the slope flattens and there is a subsequent low-mass turnover in good agreement with a Kroupa (2002) or Chabrier (2003) IMF. In Figure 2, we plot a direct comparison between the predicted CMF and observed starless/pre-stellar CMFs in different regions, which are less well-constrained than the stellar IMF but should correspond more closely with what we actually predict. The same behaviors are observed and agree well with our prediction without the need to invoke an uncertain rescaling factor (see e.g. Stanke et al. 2006; Enoch et al. 2008; Rathborne et al. 2009; Sadavoy et al. 2010; Belloche et al. 2011).

Why do HC08 recover similar behavior, given that we have shown the first-crossing and last-crossing distributions can be so different? The generating equation for the mass function in HC08 is the same as that of the original Press & Schechter (1974) derivation of the halo MF; it neglects the cloud-in-cloud problem (treating it as an ad hoc re-normalization). Modulo that renormalization, this is identical to the g_1 term in Eq. 14. This is a good approximation when the integral/ g_2 term in Eq. 14 is small and/or proportional to $f_\ell(S)$. This occurs when $dB/dS \gg B(S)/S \gg 1$; if the barrier decreases more rapidly than S (as R increases), then $\delta(R)$ for a given trajectory will evolve slowly relative to $B(R)$ and the probability of multiple crossings becomes small. In Eq. 14, the P_{01} term approaches a Dirac δ -function and the integral term $\rightarrow -f_\ell(S) + \mathcal{O}(dB/dS)^{-1}$, giving $f_\ell(S) \approx (1/2)g_1(S) + \mathcal{O}(dB/dS)^{-1}$. At scales $R/h \ll 1$, relevant for the stellar IMF, $S(R)$ is a weak function of R since most of the contributions to S come from the larger Mach numbers on larger scales, so this is satisfied.²

² This is very different from the reason that the original Press & Schechter (1974) mass function is correct to within a constant normalization, and from the nominal justification given in HC08 for assuming the same. That argument relies on a *constant* barrier ($dB/dS \equiv 0$) and applies only to the *first*-crossing distribution, for which the symmetry in P_{10} (broken in P_{01}) means that a trajectory at $\delta(S) = B(S) = B_0$ is equally likely to rise above or fall below the barrier.

This approximation would break down severely at larger scales – in fact, the HC08 mass function, applied directly to the entire galaxy disk, would include a large part of the GMC mass function, and give the result that most of the *mass* in the core MF is in $\sim 10^6 M_\odot$ “objects.” But since the derivation in HC08 specifically (and sensibly) truncates the problem before going to any large scales (focusing only on the regime $R/h \ll 1$ and $R/R_{\text{GMC}} \ll 1$), this is avoided. Also, the normalization is different, but that is essentially treated as arbitrary by the authors.

So over a limited regime, we can assume $dB/dS \gg B(S)/S \gg 1$, ignore the running of $S(R)$, and approximate the mass function as

$$\frac{dn}{dM} \sim \frac{\rho_{\text{crit}}(M)}{M^2 \sqrt{2\pi S_0}} \left| \frac{d \ln \rho_{\text{crit}}}{d \ln M} \right| \exp \left[-\frac{(\ln[\rho_{\text{crit}}/\rho_0] + S_0/2)^2}{2S_0} \right] \quad (30)$$

In the high-mass regime, the power-law slope is set by the run of ρ_{crit} with R in the turbulence-dominated regime; for R in the range such that $v_t \gg c_s$ and $R \ll h$, $S(M) \sim \text{constant}$ and $\rho_{\text{crit}} \propto R^{p-3}$, $M \propto R^p$, so the approximate analytic scaling in Eq. 30 gives a slope

$$\alpha_{\text{highmass}} \approx \frac{3(1+p^{-1})}{2} + \frac{(3-p)^2 \ln(M/M_0) - p \ln 2}{2S(M)p^2} \quad (31)$$

where $M_0 \sim \rho_0 h^3 \sim 10^5 - 10^6 M_\odot$ for typical conditions. Based on the derivation in HC08, we would expect a somewhat “lognormal-like” turnover in the high-mass end of the CMF; however, this does not self-consistently calculate the running of $S(M)$. In the exact calculation, the correction term $\propto 1/S(M)$ is already small in the range of interest (≈ -0.1 , for $S(M) \sim 10$ and $M/M_0 \sim 10^{-6} - 10^{-4}$) and higher-order corrections nearly cancel, giving a very nearly Salpeter ($\alpha \approx 2.2 - 2.4$) power-law behavior over ~ 2 dex in mass.

The turnover occurs below the sonic length, where thermal support both makes the equation of state “stiffer” and suppresses the running of the variance $S(R)$, giving $\rho_{\text{crit}} \propto R^{-2}$, $M \propto R$, so

$$\alpha_{\text{lowmass}} \approx 3 - \frac{1.5 + 4 \ln \mathcal{M}_h - 2 \ln(M/M_0)}{S(M)} \quad (32)$$

For typical parameters this becomes $\alpha_{\text{lowmass}} \sim -2 - 0.16 \ln(M/M_{\text{sonic}})$.

Our solution also allows us to predict the normalization and mass scale of the mass function, without having to make any *ad hoc* assumptions to renormalize the problem about a given scale. The CMF begins to turn over below the sonic length, $R_{\text{sonic}} = h \mathcal{M}_h^{-2/(p-1)}$, with mass $M_{\text{sonic}} \approx (4\sqrt{2}\pi/3) \mathcal{M}_h^{-2p/(p-1)} M_0 = (2/3) c_s^2 R_{\text{sonic}}/G \approx M_\odot (c_s/0.3 \text{ km s}^{-1})^2 (R_{\text{sonic}}/0.1 \text{ pc})$. The mass scale of the CMF the stellar IMF is therefore a natural consequence of Jeans collapse in a turbulent medium, with characteristic masses that depend only on the sound speed and sonic length (themselves related). This is a well-established result from both analytic work and numerical simulations (see e.g. Klessen & Burkert 2000, 2001; Bate & Bonnell 2005), and is true even if the gas is not isothermal (although our sub-sonic extrapolation is questionable in this case; see Larson 1985, 2005; Jappsen et al. 2005). There is, of course, some efficiency factor ϵ_{core} that relates the mass of a collapsing, bound protostellar “core” (which is what we actually predict) to the mass of a star. This may well depend on mass (and the thermal physics below the sonic length), which will introduce additional corrections between the IMF here and the stellar IMF (see § 5 below). However, the calculation here suggests that such corrections should be order unity, and arguments from observations and models of outflows similarly suggest a modest $\epsilon_{\text{core}} \sim 0.5$ (Matzner & McKee 2000; Stanke et al. 2006; Alves et al. 2007; Enoch et al.

2008). If constant (a significant assumption), this is comparable to the normalization uncertainty in M_{sonic} from c_s and R_{sonic} .

In Fig. 3, we plot the predicted last-crossing distribution as a function of model parameters. We compare our “default” model ($p = 2$, $\mathcal{M}_h = 30$) to one with $p = 5/3$. For otherwise equal parameters, this shifts M_{sonic} to lower absolute values, but in units of the sonic mass the behavior is qualitatively the same. The high-mass slope is nearly identical – the difference predicted by the approximate Eq. 30 or in HC08 is small to begin with, but is also largely canceled out by the second-order corrections from the proper last-crossing distribution. The low-mass turnover is much “slower,” however, since the turbulent velocity declines more slowly relative to the sound speed ($v_t \propto R^{1/3}$ instead of $R^{1/2}$ for $p = 2$), which enters into both the barrier and the run of $S(R)$. Raising the Mach number on large scales, \mathcal{M}_h , has a similar effect, and slightly steepens the high-mass slope near the turnover mass. Decreasing the Mach number steepens the turnover below M_{sonic} , and for quite low \mathcal{M}_h also begins to manifest a high-mass cutoff. These are the dominant physical effects. Changing more subtle model choices – for example, using a Gaussian window function to smooth the density field instead of a k -space tophat, make relatively little difference.

5 CAVEATS ON THE CMF-IMF CONVERSION

What we have calculated here is the mass function of self-gravitating, non-fragmenting cores at a given “snapshot” or instant, for a galaxy with fully developed non-linear turbulence. It is important to note that this is not yet the stellar IMF. As noted above, it is necessary to invoke some mean efficiency of $\sim 30\%$ in the conversion of core mass to stellar mass – presumably this comes from some combination of outflows and accretion histories, which could easily depend on mass; it is also possible that accreting protostars can be ejected from their environments, introducing a large core-to-stellar mass scatter. None of these physics are included in the current model; it may be possible to add them “on top” of the model here, but to do so it would be necessary to construct a more complex analytic model with some significant additional assumptions about how pre-stellar cores contract and grow, and how outflows affect the ambient medium.

Although within the “snapshots” here, the cores have no sub-scales which are independently self-gravitating, there can certainly be successive fragmentation on smaller scales within the cores and/or stellar accretion disks as the cores contract and form stars (which will depend on the gas thermodynamics and stellar feedback; see references above and e.g. Krumholz et al. 2009; Peters et al. 2010). Indeed this must occur, as a large fraction of stars are in binaries and high-mass stars are almost always members of higher order multiple stellar systems (Lada 2006; Zinnecker & Yorke 2007). If the multiplicity is mass-dependent (i.e. fragmentation is not scale-free), this will also change the mass spectrum from CMF to IMF. There may be some prospects of including this in future, time-dependent excursion set models (discussed below), but if fragmentation is feedback-dependent or occurs within the stellar accretion disk, following it accurately depends on physics not included in the current model.

Even if each core forms a fixed fraction of its mass into a fixed number of stars, the timescales for it to do so may be different. What the IMF really samples is the relative “formation rate” of stars of a given mass; so if the timescale for collapse of massive cores is much longer than the timescale for collapse of low-mass cores, this can significantly change the shape of the IMF relative to the CMF (see the discussion in Clark et al. 2007). At high masses

$M \gtrsim M_{\text{sonic}}$, we do not expect the dependence of collapse timescale on mass to strongly change our results. For $R \gtrsim R_{\text{sonic}}$ and $R \ll h$, the characteristic collapse time for cores scales as $\sim t_{\text{dyn}} \propto \rho_{\text{crit}}^{-1/2} \propto R/v_t \propto R^{1/2} \propto M^{1/4}$. If the rate of star formation simply scales as $\propto n_{\text{core}}/t_{\text{collapse}}$, this implies the bright end of the stellar IMF will be steeper than that of the CMF predicted here by $M^{-1/4}$. This is not a negligible correction, but it is also not very large (comparable to the difference between $p = 5/3$ and $p = 2$). Moreover, for $p = 2$ it actually goes in the “right” direction: the CMF slope predicted (with second-order corrections, $\alpha \sim 2.15 - 2.2$) is slightly more shallow than the canonical Salpeter slope, so this would bring the predicted IMF slope closer to observations. However, at low masses ($\ll M_{\text{sonic}}$), this effect is more important: $t_{\text{dyn}} \propto R/c_s \propto R \propto M$, so the timescale correction can significantly modify the CMF-IMF relation. But in this regime, we already noted that our predictions are much more sensitive to the turbulent spectrum, and our simplifying assumption that the gas is isothermal, while introducing negligible corrections at $R > R_{\text{sonic}}$, can have large effects on CMF in the sub-stellar ($R \ll R_{\text{sonic}}$) regime (see Hennebelle & Chabrier 2009). We therefore caution that while collapse times are critical to the CMF-IMF conversion at low masses, the gas thermodynamics is likely to be an equal or greater source of uncertainty (given the simplicity of our derivation here).

6 DISCUSSION & CONCLUSIONS

We have applied the excursion set model of the ISM, developed in H11, to predict the mass spectrum of star-forming cores and, by (admittedly less certain) extrapolation, the stellar IMF. We note that the density field smoothed on a scale R about a random point \mathbf{x} in the ISM, $\delta(\mathbf{x}, R)$ may be self-gravitating on many scales. The largest of these scales defines the “first crossing distribution,” which we show in H11 should be associated with the distribution of GMCs. If it is also self-gravitating on smaller scales, then this “parent” scale is not part of the core MF or stellar IMF, but will fragment into smaller units that collapse first: rather, the CMF should be associated with the “last crossing distribution,” or the mass function defined on the *smallest* scales on which systems are self-gravitating. To our knowledge, this has not previously been studied in cosmological or ISM applications. This can be determined in a standard Monte Carlo excursion set approach, but we also derive the exact analytic solution for an arbitrary collapse threshold. We use this to predict the CMF, and find it agrees very well with that observed. The high-mass slope emerges as a consequence of turbulent support/fragmentation and is very close to a power-law over ~ 2 dex, and very insensitive to the properties of turbulence for reasonable power spectra. The slope flattens at the sonic length/mass, $\sim c_s^2 R_{\text{sonic}}/G$, as thermal pressure makes the effective equation of state more “stiff.” The shape of this turnover is robust, but exactly how rapidly it occurs (in units of mass) depends on the Mach number and turbulent spectral shape.

Our calculation supports the conclusions of HC08, who derive the same behavior from a simpler “collapsed fraction” argument, and do not attempt to calculate the variance in the density field or disk-scale effects. In many ways, the derivation here is related to that work as that in Bond et al. (1991) is related to Press & Schechter (1974). We have provided a formal mathematical justification, and exact solution, for the approximate mass function therein. Moreover we provide a means to calculate the normalization (of both space density and mass scale) and variance beginning at the parent disk scale, which removes many ambiguities. And

incorporating the argument into the full excursion set framework makes possible many additional calculations.

We stress that the model used here to derive the CMF is *exactly* the same as that used in H11 to predict the properties of the GMC population and large-scale ISM structure. The only difference is that here we examine the last, instead of first, crossing distribution. Thus, beginning at the scale of an entire galactic disk, with the only “free parameter” being the turbulent spectrum, we derive first the distribution of GMCs, and *simultaneously* the MF of cores on much smaller scales near the sonic length, within those GMCs. This is, to our knowledge, the first analytic model that simultaneously predicts the CMF/IMF and large-scale ISM properties – both in remarkably good agreement with observations.

There are a number of obvious extensions to our calculation. With a rigorous definition of the last-crossing distribution, it is straightforward to predict other properties derived for the GMC population in H11: the core size-mass and linewidth-size relations, the distribution of “voids” or “bubbles,” the collapse rate of bound structures (and rate at which new mass is “supplied” into cores), and the dependence of these properties on turbulent spectral index, Mach number, gas thermal properties, and more. With a well-defined f_ℓ (the last-crossing distribution; Eq. 14) it is possible to calculate the correlation function of individual stars and clustering properties of star formation.

In H11, we also show how the excursion set formalism can be used to construct a Monte Carlo “merger/fragmentation tree,” analogous to extended Press-Schechter halo merger trees, with which it is possible to follow the time evolution of the ISM and GMC populations and build semi-analytic models for the same. Since the last-crossing is determined for all trajectories in the Monte Carlo formalism, it is straightforward to extend this to sample the IMF in a fully rigorous time-dependent manner, as a function of properties in different GMCs. With this formalism, GMCs, once bound, can be allowed to depart from the background flow, and this can in turn be allowed to change the CMF and ultimately the IMF. The IMF calculation could, in turn, be used to determine the per-GMC SFR and stellar mass distribution, which then informs whatever model of feedback is used to evolve the clouds themselves. One might imagine a model in which, for example, the GMC remains bound until a sufficient number of sub-regions have experienced last-crossing at a scale sufficiently large to form O-stars, which then dissociate the cloud. This also provides a means to generalize calculations such as that in Krumholz & McKee (2005) to rigorously derive the star formation *rate*, without having to assume an ad hoc collapse timescale $\sim t_{\text{dyn}}$.

It is also possible to follow time-dependent fragmentation. One concern with our “instantaneous” calculation (which essentially calculates last-crossing for the galaxy at a “snapshot” in time) is that a non-negligible amount of mass has its last crossing at scales much larger than any single star: see e.g. the overlap in the high-mass f_ℓ and low-mass tail of the first-crossing or GMC mass function in Fig. 1. In a fully time-dependent model though, these regions would require at least ~ 1 dynamical time to contract, which amounts to many dynamical times for the denser sub-regions of the cloud. In this time, therefore, a large number of sub-regions might cross below the barrier – this is a purely analytic means to calculate time-dependent fragmentation of collapsing objects. This is likely to resolve the “problem” of these otherwise high-mass objects, but also to steepen the high-mass end of the predicted IMF relative to the CMF. Extension of our models to a fully time-dependent formulation may also provide a means to address the timescale corrections and fragmentation processes discussed in § 5, which are

critical to understand the relation between CMF predicted here and stellar IMF. Including the effect of outflows is, however, non-trivial, and will require the introduction of fundamentally new physics in the models.

ACKNOWLEDGMENTS

We thank Chris McKee and Eliot Quataert for helpful discussions during the development of this work. We also thank our referee, Ralf Klessen, as well as Patrick Hennebelle, Gilles Chabrier, and Alyssa Goodman for a number of suggestions and thoughtful comments. Support for PFH was provided by NASA through Einstein Postdoctoral Fellowship Award Number PF1-120083 issued by the Chandra X-ray Observatory Center, which is operated by the Smithsonian Astrophysical Observatory for and on behalf of the NASA under contract NAS8-03060.

REFERENCES

- Alves, J., Lombardi, M., & Lada, C. J. 2007, *A&A*, 462, L17
 Bate, M. R., & Bonnell, I. A. 2005, *MNRAS*, 356, 1201
 Belloche, A., Schuller, F., Parise, B., André, P., Hatchell, J., Jørgensen, J. K., Bontemps, S., Weiß, A., Menten, K. M., & Muders, D. 2011, *A&A*, 527, A145
 Bond, J. R., Cole, S., Efstathiou, G., & Kaiser, N. 1991, *ApJ*, 379, 440
 Brunt, C. M., Heyer, M. H., & Mac Low, M.-M. 2009, *A&A*, 504, 883
 Chabrier, G. 2003, *PASP*, 115, 763
 Chabrier, G., & Hennebelle, P. 2011, *A&A*, 534, A106
 Clark, P. C., Klessen, R. S., & Bonnell, I. A. 2007, *MNRAS*, 379, 57
 Donkov, S., Veltchev, T. V., & Klessen, R. S. 2011, *MNRAS*, 418, 916
 Elmegreen, B. G., & Scalo, J. 2004, *ARA&A*, 42, 211
 Enoch, M. L., Evans, II, N. J., Sargent, A. I., Glenn, J., Rosolowsky, E., & Myers, P. 2008, *ApJ*, 684, 1240
 Federrath, C., Klessen, R. S., & Schmidt, W. 2008, *ApJL*, 688, L79
 Hennebelle, P., & Chabrier, G. 2008, *ApJ*, 684, 395
 —. 2009, *ApJ*, 702, 1428
 —. 2011, *ApJL*, 743, L29
 Hopkins, P. F. 2011, *MNRAS*, in press, arXiv:1111.2863 [astro-ph]
 Inutsuka, S.-i. 2001, *ApJL*, 559, L149
 Jappsen, A.-K., Klessen, R. S., Larson, R. B., Li, Y., & Mac Low, M.-M. 2005, *A&A*, 435, 611
 Klessen, R. S., & Burkert, A. 2000, *ApJS*, 128, 287
 —. 2001, *ApJ*, 549, 386
 Kroupa, P. 2002, *Science*, 295, 82
 Krumholz, M. R., Klein, R. I., McKee, C. F., Offner, S. S. R., & Cunningham, A. J. 2009, *Science*, 323, 754
 Krumholz, M. R., & McKee, C. F. 2005, *ApJ*, 630, 250
 Lada, C. J. 2006, *ApJL*, 640, L63
 Larson, R. B. 1985, *MNRAS*, 214, 379
 —. 2005, *MNRAS*, 359, 211
 Mac Low, M.-M., & Klessen, R. S. 2004, *Reviews of Modern Physics*, 76, 125
 Matzner, C. D., & McKee, C. F. 2000, *ApJ*, 545, 364
 McKee, C. F., & Ostriker, E. C. 2007, *ARA&A*, 45, 565
 Nordlund, Å. K., & Padoan, P. 1999, in *Interstellar Turbulence*; Cambridge University Press, ed. J. Franco & A. Carraminana (Cambridge, UK: Cambridge University Press), 218–
 Ossenkopf, V., & Mac Low, M.-M. 2002, *A&A*, 390, 307

- Ostriker, E. C., Gammie, C. F., & Stone, J. M. 1999, *ApJ*, 513, 259
- Padoan, P., & Nordlund, Å. 2002, *ApJ*, 576, 870
- Padoan, P., Nordlund, A., & Jones, B. J. T. 1997, *MNRAS*, 288, 145
- Passot, T., & Vazquez-Semadeni, E. 1998, *PhRvE*, 58, 4501
- Peters, T., Klessen, R. S., Mac Low, M.-M., & Banerjee, R. 2010, *ApJ*, 725, 134
- Press, W. H., & Schechter, P. 1974, *ApJ*, 187, 425
- Price, D. J., Federrath, C., & Brunt, C. M. 2011, *ApJL*, 727, L21
- Rathborne, J. M., Lada, C. J., Muench, A. A., Alves, J. F., Kainulainen, J., & Lombardi, M. 2009, *ApJ*, 699, 742
- Sadavoy, S. I., Di Francesco, J., Bontemps, S., Megeath, S. T., Rebull, L. M., Allgaier, E., Carey, S., Gutermuth, R., Hora, J., Huard, T., McCabe, C.-E., Muzerolle, J., Noriega-Crespo, A., Padgett, D., & Terebey, S. 2010, *ApJ*, 710, 1247
- Scalo, J., & Elmegreen, B. G. 2004, *ARA&A*, 42, 275
- Scalo, J., Vazquez-Semadeni, E., Chappell, D., & Passot, T. 1998, *ApJ*, 504, 835
- Stanke, T., Smith, M. D., Gredel, R., & Khanzadyan, T. 2006, *A&A*, 447, 609
- Vazquez-Semadeni, E. 1994, *ApJ*, 423, 681
- Veltchev, T. V., Klessen, R. S., & Clark, P. C. 2011, *MNRAS*, 411, 301
- Zhang, J., & Hui, L. 2006, *ApJ*, 641, 641
- Zinnecker, H., & Yorke, H. W. 2007, *ARA&A*, 45, 481